

Vanadium Dioxide: Metal-Insulator Transition, Electrical Switching and Oscillations. A Review of State of the Art and Recent Progress

Alexander Pergament^{1,2,*}, Aurelian Crunteanu¹, Arnaud Beaumont¹,
Genrikh Stefanovich², and Andrey Velichko²

¹ *XLIM Research Institute, UMR7252 CNRS/ Université de Limoges, LIMOGES Cedex FRANCE*

² *Department of Physical Engineering, Petrozavodsk State University, PETROZAVODSK Republic of Karelia RUSSIA*

Abstract. Vanadium dioxide is currently considered as one of the most promising materials for oxide electronics. Both planar and sandwich thin-film metal/oxide/metal devices based on VO₂ exhibit electrical switching with an S-shaped I - V characteristic, and this switching effect is associated with the metal-insulator transition (MIT). In an electrical circuit containing such a switching device, relaxation oscillations are observed if the load line intersects the I - V curve at a unique point in the negative differential resistance region. All these effects are potentially prospective for designing various devices of oxide electronics, such as, particularly, elements of dynamical neuron networks based on coupled oscillators. In this paper, we present a brief review of the state of the art and recent advances in this though only freshly emerged, but exciting and rapidly developing field of research. We start by describing the experimental facts and theoretical models, mainly on the basis of the Mott MIT in vanadium dioxide as a model object, of the switching effect with especial emphasis on their applied potentialities for oxide electronics, and then turn to our recent results concerning synchronization of an array of coupled oscillators based on VO₂ switches. In conclusion, we try to formulate an outlook on how these findings can contribute to the future development of bio-inspired neuromorphic devices implementing the associative memory function, that is, non-Boolean computing with artificial neural networks^{**}.

Keywords: metal-insulator transition, switching, relaxation oscillations, coupled oscillators, artificial neural networks.

1. Introduction

The unprecedented diversity of physical properties exhibited by transition metal oxides offers immense prospects for various electronic applications. The term “oxide electronics” have emerged not so long ago in the everyday-life of scientific literature, but already firmly taken its place [1]. The point is that the modern IT revolution is based on technological progress which enables an exponentially growing enhancement of the performance of electronic devices. During all the history of the development of electronic components, from a vacuum diode to modern highly integrated ICs with nanometer scale of individual elements, the question of the physical limitations on the further progress in this area arose repeatedly.

^{*}) Corresponding author, e-mail: aperg@psu.karelia.ru

^{**}) This work was presented as an oral talk at the Energy Materials and Nanotechnology (EMN) Meeting on Computation and Theory, Istanbul (Turkey) 9-12.11.2015, <http://emnmeeting.org/theory/program/>

After the invention of an IC by J. Kilby and R. Noyce in 1958 [2], the amount of devices is continuously increased from 1960s by means of device miniaturisation, following the so-called Moore's law. In recent years, the issue of constraints for standard Si-based electronics has been widely discussed in the scientific literature, which is primarily associated with the possibility of further scaling toward nano-size. In this regard, in the 2007 edition of The International Technology Roadmap for Semiconductors (ITRS, <http://www.itrs.net>), a new section has appeared, namely "Emergent Research Device Materials", which indicates the need to develop a new generation of devices based on new physical principles [3].

Alternative approaches are based on another mechanism (as compared to the field effect in Si CMOS FETs) or even on a drastic change in computational paradigm or architecture (quantum computers, neuroprocessors). Amongst the approaches utilizing new physical mechanisms, one can list, for example, spintronics, superconducting electronics, single-electronics, molecular electronics, soletronics (single atom electronics) [1]. One of such novel directions, oxide electronics, is based on the idea of application of unique properties and physical phenomena in strongly correlated transition metal oxides (TMO). Metal-insulator transition (MIT) [4] belongs to the class of the aforementioned phenomena, and many TMOs, e.g. vanadium dioxide, undergo MITs as functions of temperature or electric field [4, 5].

Vanadium dioxide is currently considered as one of the most promising materials for oxide electronics. Both planar and sandwich thin-film MOM devices based on VO₂ exhibit electrical switching with an S-shaped I - V characteristic, and this switching effect is associated with the MIT. In an electrical circuit containing such a switching device, relaxation oscillations are observed if the load line intersects the I - V curve at a unique point in the negative differential resistance (NDR) region. All these effects are potentially prospective for designing various devices of oxide electronics, such as, particularly, the Mott-FET (field effect transistor based on the Mott MIT material) [5] or elements of dynamical neuron networks based on coupled oscillators [6].

In this brief review we discuss the state of the art and recent advances in this though only freshly emerged, but exciting and rapidly developing field of research. We start by describing the experimental facts and theoretical models, mainly on the basis of the Mott transition in vanadium dioxide as a model object, of the switching effect with especial emphasis on their applied potentialities for oxide electronics, and then turn to our recent results concerning synchronization of an array of coupled oscillators based on VO₂ switches. The latter findings are of crucial importance for future development of bio-inspired neuromorphic devices implementing the associative memory function, that is, non-Boolean computing with artificial neural networks [6, 7].

2. MIT and electronic switching in VO₂

2.1. Overview of experimental data

Since the discovery of the MIT in VO₂ [8], there has been a lot of interest in this kind of phase transition, as it is accompanied by a large change in the electrical resistivity and optical properties. This transition occurs at $T_t = 340$ K (Fig.1). In single crystals, the resistivity change reaches a factor of 10^5 over a temperature range of 0.1 K [9]. Hysteresis associated with this transition is of about 2 K. The conductivity jump and the narrowness of the hysteresis loop is a very good indication of how close the stoichiometry is to VO₂. Small deviations destroy the sharpness of the transition and increase the hysteresis width. The crystalline state of the material has an influence too: polycrystalline material will have a broader transition than single crystals. The transition temperature also depends on the crystalline state and oxygen non-stoichiometry. As a rule, the MIT in VO₂ is to a certain degree suppressed in thin films as compared to single crystals.

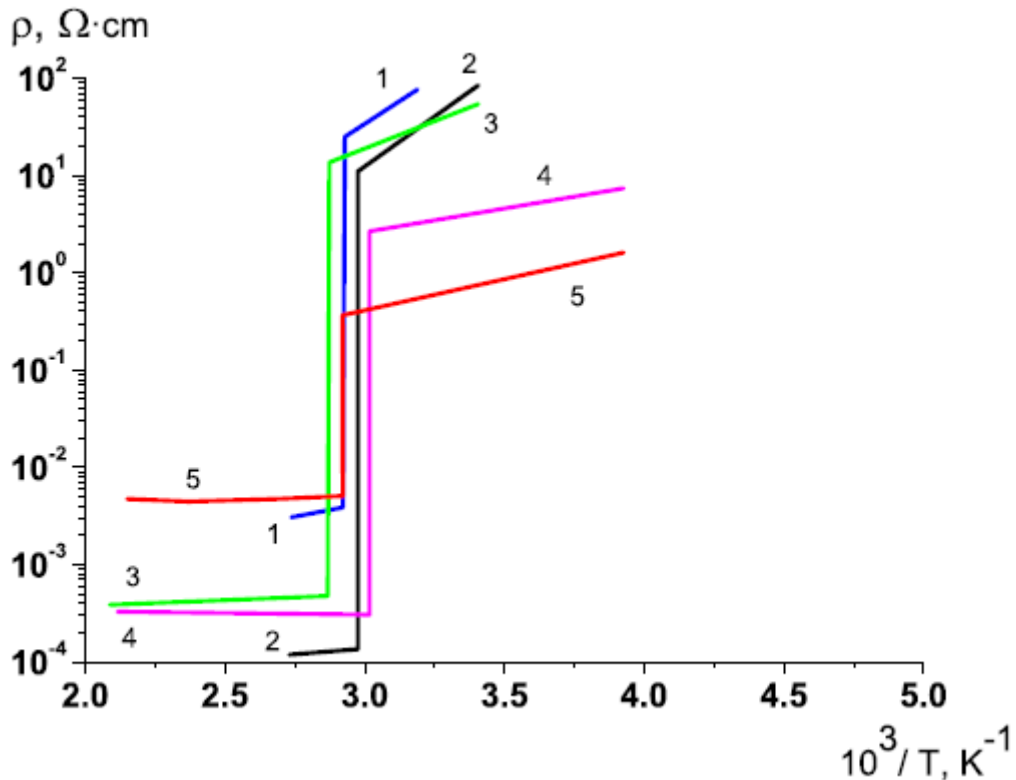


Fig. 1. Resistivity of VO₂ single crystals along the c axis as a function of reciprocal temperature (1 - 5: data from different works for samples of various degrees of perfection; for references see [4], 1st edition of 1974) [5].

At high temperatures, vanadium dioxide has a rutile-type structure with vanadium atoms equally spaced along the corresponding c_r -axis. At the transition to the low-temperature state, these vanadium atoms pair along the c_r -axis with a slight twist which leads to a monoclinic symmetry. The gap in the insulating low-temperature phase is about 0.7-1.0 eV (depending on stoichiometry and other factors).

Despite the many efforts made towards obtaining an understanding of their electronic behavior, the vanadium oxides still pose many open questions. This fully applies to VO₂ as far as the nature of transition is concerned. Some authors related its phase transition to a Mott-Hubbard scenario, whereas others attributed it to electron-phonon coupling (a Peierls mechanism) on the basis of the crystal symmetry change. In the recent monograph [10], it is stated that the metal-insulator transition in VO₂ has a combined nature, having the features of both Mott and Peierls transitions.

Nonetheless, many experimental facts indicate that the transition might be initiated by an increase in the free charge carrier density (without heating to $T = T_t$ and without affecting the lattice, i.e. not under, for example, doping or pressure) under photo-generation [11], injection [12], or high-field generation at switching [13]. These results evidence that the electron-electron interaction is of importance for a correct description of the transition. This is supported by studies of the MIT in thin films of amorphous vanadium dioxide obtained by anodic oxidation [14, 15].

It should be emphasized however that the question about the MIT mechanism in VO₂, posed as “either Mott or Peierls transition” [16], has no sense because, actually, this mechanism is essentially dual [17]. Meanwhile, one should be aware of the fact (and take this fact into account when analyzing the capabilities of VO₂-based electronic devices) that the initiating mechanism is still the correlation-driven electronic Mott transition [5].

In two-terminal MOM devices with vanadium dioxide, electrical switching due to MIT is observed [18-27] (Fig. 2). This switching effect is described in terms of the current-induced Joule heating of the sample up to $T = T_t$, which has been confirmed by the direct IR-radiation measurements of the switching channel temperature [20, 27]. In these early works, switching has been observed in single crystals [21], planar thin-film devices [19, 20, 27], as well as in vanadate glasses [22, 23], VO₂-containing ceramics [26], V₂O₅-gel films [24, 25] and anodic oxide films on vanadium [18]. When as-prepared samples do not consist of pure vanadium dioxide, preliminary electroforming is required, resulting in the formation of the VO₂ containing channel [18, 22, 24]. For such samples the threshold voltage decreases with temperature and reaches zero at $T \sim T_t$.

In this case, the switching mechanism is well described by a simple thermal model often termed as the “model of critical temperature” [19], provided that the ambient temperature T is not much lower than T_t :

$$V_{th} \sim (T - T_t)^{1/2}, \quad (1)$$

that is, the squared threshold voltage linearly tends to zero at $T \rightarrow T_t$, see Fig. 2(c).

However, at a sufficiently low temperature, and in sandwich thin-film nanostructures (that is, in high electric fields), the possible influence of electronic effects on the MIT should be taken into account. A field-induced increase in charge carrier density will act to screen Coulomb

interactions, leading to the elimination of the Mott-Hubbard energy gap at $T < T_t$ [5, 12, 13]. This non-thermal (electronic) mechanism of switching in VO₂ is considered in the next section.

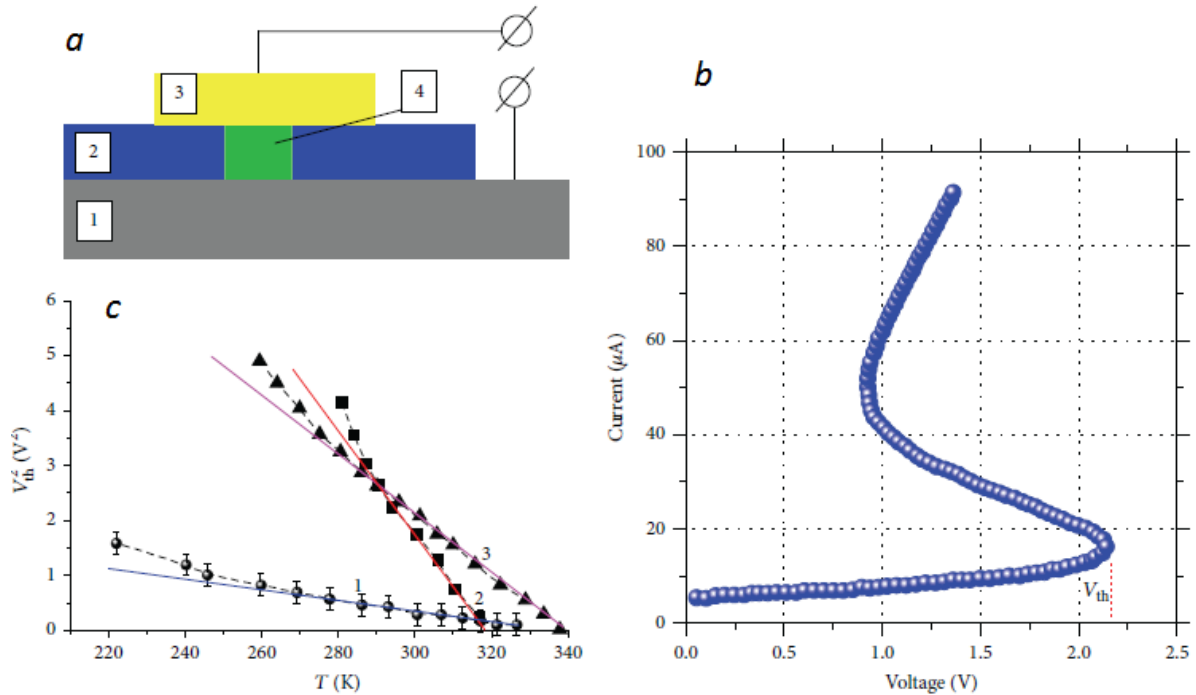


Fig.2. (a) The sandwich switching structure (schematic) based on anodic vanadium oxide (AVO) [5]: 1 – vanadium metal substrate, 2 – anodic oxide film, 3 – Au electrical contact, 4 – VO₂ switching channel; (b) the I - V characteristic after electroforming for one of the samples at room temperature. (c) Squared threshold voltage as a function of temperature for vanadium oxide-based switch: 1, 2, 3 – three different samples.

Finally, it should be noted that although the switching effect in vanadium dioxide has long been known, recently this problem has received considerable attention once again, primarily due to the promising potential applications in emerging oxide electronics (what these applications are, we have briefly mentioned in the introduction, and will discuss in more detail below in Section 3). In this regard, a large and ever-growing number of works dedicated to switching in vanadium dioxide have been published at present. Without a possibility to analyze or even mention all of them here, we refer to the recent reviews [5, 28, 29] where the reader can find corresponding discussions.

2.2. Electronically-driven switching in VO₂

Application of an electric field to a Mott insulator, taking also into account the current flow, will result in both the thermal generation of additional carriers due to the Joule heat, and in the field-induced generation. The latter is due to the autoionization caused by the Coulomb

barrier lowering – a phenomenon analogous to the Poole-Frenkel effect [13], when the density depends on the electrical field strength E as follows:

$$n = N_0 \exp\left(-\frac{W - \beta\sqrt{E}}{kT}\right), \quad (2)$$

where N_0 is a constant independent of the field and only slightly dependent on temperature, W – the conductivity activation energy, and $\beta = (e^3/\pi\epsilon_\infty\epsilon_0)^{1/2}$ – the Poole-Frenkel constant; ϵ_∞ is the high-frequency dielectric permittivity.

When the total concentration of free carriers reaches the value of $n = n_c$, the transition into the metal state, i.e. switching of the structure into the ON-state, occurs. In a material with the temperature-induced MIT, like VO_2 , this switching (in a relatively low field) occurs just due to the heating of the switching channel up to $T = T_t$ according to the critical temperature model, equation (1). The above mentioned value of n_c is determined by the Mott criterion:

$$a_H n_c^{1/3} \approx 0.25, \quad (3)$$

where $a_H = \epsilon\hbar^2/m^*e^2$ is the effective Bohr radius, m^* – the effective mass of charge carriers and ϵ – the static dielectric permittivity.

In the paper [13], it has been reported on the switching mechanism in vanadium dioxide. This mechanism is shown to be based on the electronically-induced Mott insulator-to-metal transition occurring in conditions of the non-equilibrium carrier density excess in the applied electric field. The model has been developed on the basis of the measurements of I - V characteristics of M/AVO/M sandwich structures (Fig. 3). It has been shown that, as the electric field strength increases, the transition temperature (i.e. the temperature at which the switching

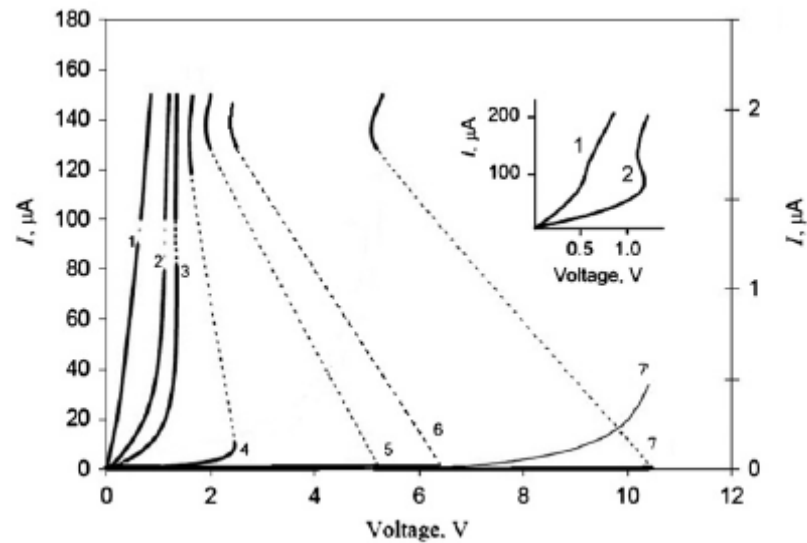


Fig. 3. I - V curves at different temperatures in the range 15 – 300 K [13]. T_0 : (1) 293 K, (2) 241 K, (3) 211 K, (4) 144 K, (5) 91 K, (6) 70 K, (7) 15 K. Curve (7') represents the OFF state for $T_0 = 15$ K (right-hand current axis), and the inset shows curves (1) and (2) on a large scale.

event inside the channel occurs) decreases. Numerical simulation of the free charge carrier density has been made (Fig. 4, curve 1) using the relation $\sigma = ne\mu$, where σ is the channel conductivity obtained from the data of Fig. 3, and $\mu = 0.5 \text{ cm}^2 \text{ V}^{-1} \text{ s}^{-1}$ is the mobility of electrons in vanadium dioxide. One can see that at $T_0 < 200 \text{ K}$ ($E > 10^5 \text{ V cm}^{-1}$), for $\mu = \text{const}$, the value of n becomes less than the critical Mott density n_c in equation (3), which for vanadium dioxide has been estimated to be $n_c \sim 3 \cdot 10^{18} \text{ cm}^{-3}$ (dotted line in Fig. 4).

If however we take into account the temperature dependence of the mobility, this discrepancy can be eliminated [30]. It has been shown [31] that the conductivity of a VO_2 switching channel can be written as

$$\sigma \sim \frac{1}{T^{3/2}} \exp(-E_a/k_B T + k_B T/\xi), \quad (4)$$

where E_a is the conductivity activation energy, and ξ is a constant of the small polaron hopping conduction theory which takes into account the influence of thermal lattice vibrations onto the resonance integral [31]. In equation (4), the first term in the exponent is responsible for the band conduction, whereas the second one characterizes the temperature dependence of the hopping mobility. Therefore the data on $n_m(T)$ (Fig. 4, curve 1) should be corrected by means of division by a factor corresponding to the mobility temperature dependence, which could be obtained from Eq.(4) [30]:

$$\mu(T) \sim (1/T) \exp(k_B T/\xi). \quad (5)$$

These corrected values of n_m are presented by curve 2 in Fig. 4. One can see that, within an order of magnitude, these values correspond to the Mott critical concentration.

Thus, the switching mechanism is based on the electronically-induced Mott metal-insulator transition taking into consideration the dependence of the carrier density on electric field, equation (2), and the temperature dependence of the electron mobility in VO_2 , equation (5).

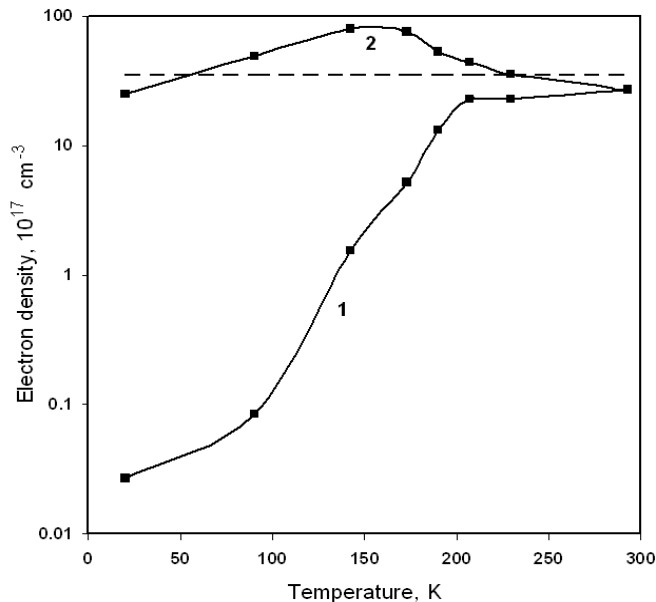


Fig. 4. Maximum electron density in the switching channel as a function of ambient temperature; in fact, n_m depends on the threshold electric field E_{th} , and the latter, in turn, depends on T_0 . The calculations are made for the cases of $\mu = \text{const}$ (curve 1) and $\mu \sim T_m^{-1} \exp(k_B T_m/\xi)$ (curve 2). Here T_m ($\neq T_0$) is the temperature in the channel centre calculated on the basis of mathematical simulating [13].

2.3. Relaxation oscillations in circuits with VO₂ switches

In a scheme with an S-NDR device, at a high enough d.c. bias (V_0), relaxation oscillations are observed if the load line intersects with the I - V curve at a unique point in the NDR region (Fig. 5) [5]. The frequency of this oscillation ($f_r = 1/T_r$) depends on the threshold parameters and, consequently, it depends on external parameters, e.g. on temperature and pressure. Sensors with the frequency output have a number of evident advantages: high sensitivity and stability, convenience of processing of a signal, capability of remote measurements, low noise susceptibility.

The expression for T_r one can obtain from the known exponential voltage vs. time dependence for the charging of a capacitor:

$$V(t) = V_0[1 - \exp(-t/\tau)], \quad (6)$$

whence:

$$T_r = \tau \ln \frac{V_0 - xV'}{V_0 - xV_{th}}, \quad (7)$$

where $x = (R_L/R_0)+1$, $\tau = R_L C/x$ and R_0 is the OFF-state resistance of the switch [32]. In the absence of a parallel-connected capacitor, C is the switch self-capacitance determined by its geometrical dimensions and the value of $\varepsilon(f, T_0)$ of VO₂. Fig. 5(d) shows the experimental temperature dependencies of the oscillation frequency for three M/AVO/M samples.

Much attention in the literature is also paid to the noise and chaotic dynamics at switching in vanadium dioxide, primarily because of their importance in bolometric applications [33-35]. Particularly, generation of stochastic oscillations has been observed in [36]. For sufficiently large amplitudes of the periodic signal, a new nonlinear effect in stochastic resonance has been found. In these experiments, a sin-wave generator was connected in series with the DC source. In the presence of a weak internal noise, it is possible to observe the phenomenon of locking the mean switching frequency, see Fig. 6. At first, the frequency of switching coincides with the signal frequency Ω . Then, as the Ω increases over the natural system frequency f_r , the switching period becomes twice as greater in comparison with $T_L=1/\Omega$ (Fig. 6 (c)). Between these two states, a chaotic regime appears with the phase diagram of I and V shown in Fig. 6(b). Thus, there exist two limit cycles, between which the phase trajectory moves chaotically and fills in the space between them. As the frequency continues to increase, the described process is repeated, i.e. the oscillations with $T = NT_L$ ($N = 3, 4, 5 \dots$) appear. The same transition between different oscillating behaviors is observed when varying the amplitude of the sin-wave signal or the DC voltage V_0 , not only the frequency Ω . The above-described chaotic behavior represents the intermittent chaos [36], i.e. the random transitions between two limit cycles (attractors) during the period-adding process.

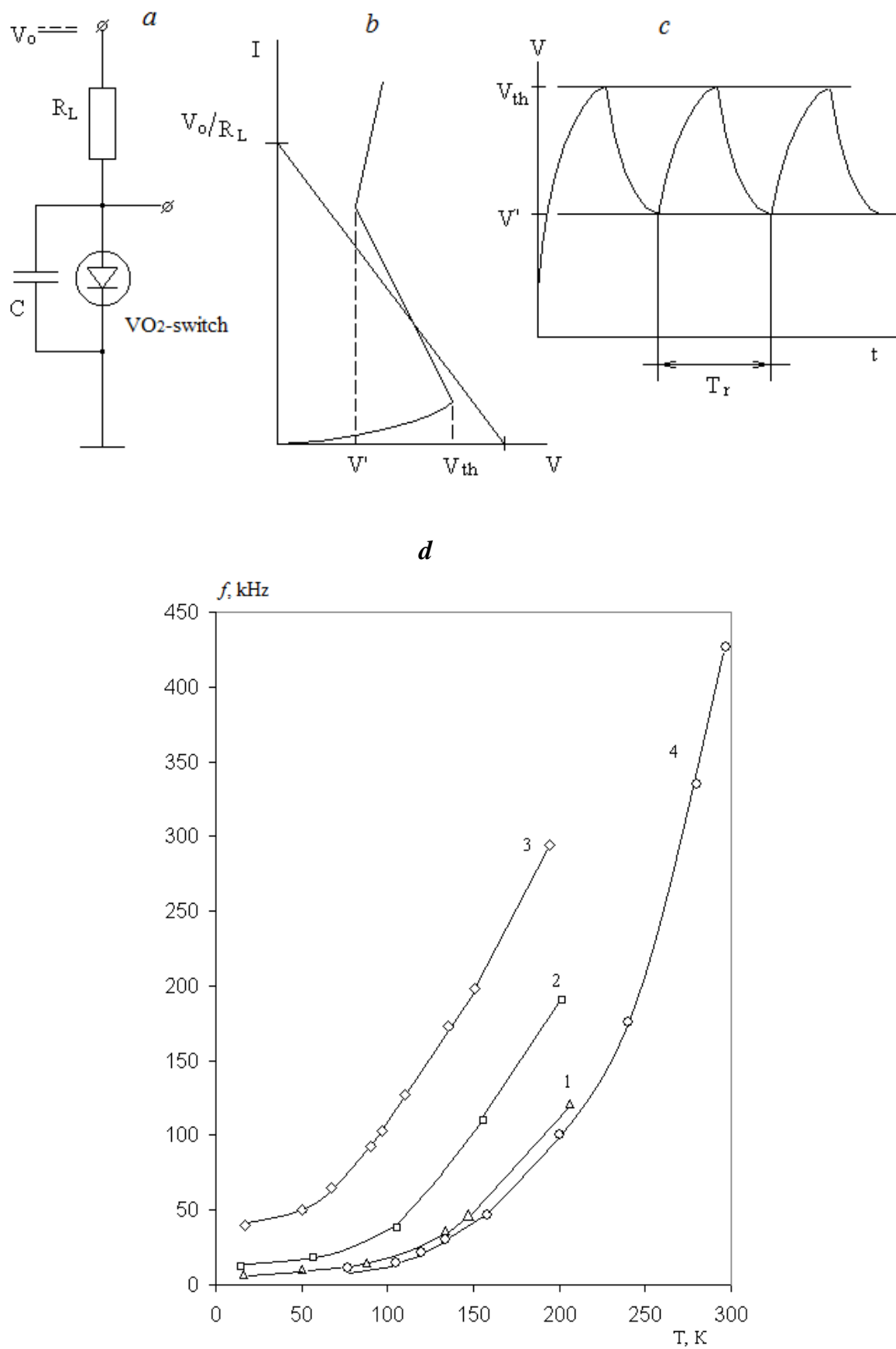


Fig. 5. Relaxation oscillations: (a) electrical circuit, (b) schematic $I-V$ curve and load line, and (c) output signal oscillogram. (d) Temperature dependences of f_r for three samples with different threshold voltages (at $T = 100$ K): $V_{th} = 4.4$ V (1, 2), 1.64 B (3) and 7.7 V (4). The values of V_0 and R_L are: 80 V and 1.4 M Ω (1); 95 V and 1 M Ω (2); 40 V and 0.6 M Ω (3); 100 V and 1.05 M Ω (4).

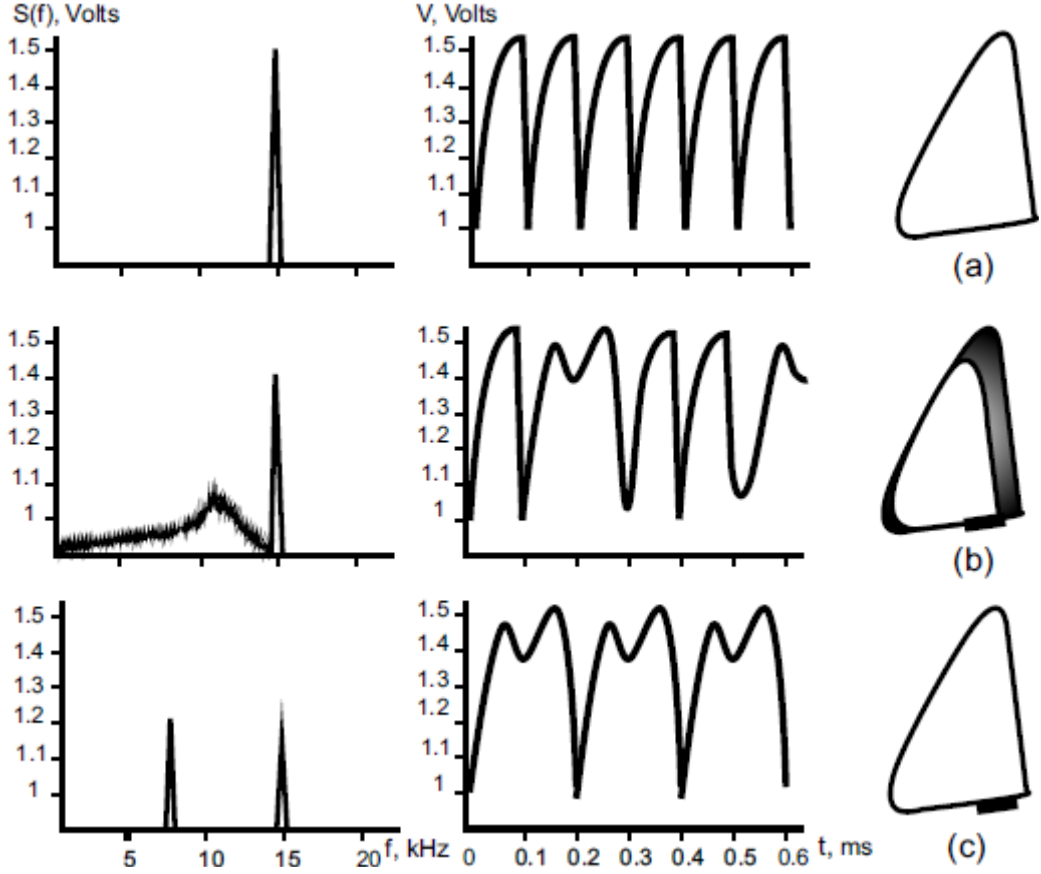


Fig. 6. Oscillation spectra, voltage oscillograms, and phase portraits (I - V orbits) for different values of Q : (a) $Q1$, frequency locking; (b) $Q2$, chaotic oscillations; and (c) $Q3$, period doubling. $Q1 < Q2 < Q3$ [36].

Electrical self-oscillations across out-of-plane threshold switches based on VO_2 have also been studied in [6]. It is argued there that, beside integration as inverters and oscillators in high-speed circuits, a prospective potential application of these results may be connected with the parallel production of periodic signals in large-scale integrated circuits, analogous to the action potentials in neural architectures. In the next section, we present our results concerning synchronization of a pair of coupled oscillators based on VO_2 switches.

3. Coupled VO_2 oscillators

3.1. Background

Nowadays information processing is widely performed by CMOS circuits based on Boolean logics. The amount of devices is continuously increased from 1960s by means of device miniaturization, following the so-called Moore's law [37]. The pace of the miniaturization is set by the ITRS roadmap, which accounts for cost-effectiveness of the R&D efforts required to sustain it. This cost-effectiveness has recently been impacted by fundamental issues such as quantum effects but also by a decrease and a diversification of the demand and by the increase of

the cost of the equipment needed for large-scale fabrication of nanoscale devices. Fundamental aspects have been partially and temporally circumvented by the use of new device architectures and new materials [38]. However, the miniaturization pace of CMOS devices has slowed down despite the considerable efforts made by the scientific community and the study of nanoscale emerging devices able to assess the tasks of CMOS transistors has flourished [39].

One of the main hurdle CMOS devices have to tackle to keep on the miniaturisation is power consumption. On the other hand, it appears difficult to fabricate alternative nanoscale device that can compete with CMOS concerning power consumption while showing similar computing efficiency once assembled into a circuit. This calls the paradigm of information processing into question: is it only the CMOS technology that reaches its limit or is it Boolean logics [40]? Dropping Boolean logics for processing information would have a very interesting benefit: one could imagine systems where information is not carried by electric charge, the motion of which is intrinsically dissipative. This has already been proposed for Boolean logics (e.g. with electron spins) but many more information carriers could be envisaged if Boolean logics was not mandatory, in particular analog information carriers could be used. The question to know if analog information carriers are less dissipative than electrical charge is still open but they would enable to drop a more global paradigm which is called Von Neumann computation. It is the base of all actual information processing systems and it schematically consists in performing sequential commands, which is well suited to Boolean logics. It is also known to have a limit coined as “Von Neumann bottleneck” related to the sequential nature. The multi-core trend in microprocessors may indicate that this bottleneck is reached and that it is time to think of intrinsically parallel computation architectures.

This context led some research groups to look into how a brain processes information in order to try to mimic it with electronic circuits. Since there are different kinds of neurons operating with different mechanisms, many bioinspired computation architectures have been proposed [41]. Among them oscillatory neural networks (ONNs) have attracted much attention because the basic bricks are oscillators. An oscillator may be fabricated by many different ways with common electronic devices, most of the time with quite large circuits. However, it has been shown that a simple capacitor made of an insulator featuring a MIT can oscillate between a high-resistance and a low-resistance state when an appropriate bias is applied to it, as is discussed in Section 2.3 above and in the works [42-44]. This means that the basic block of ONNs can be very small, which explains the attractivity of such circuits for large integration.

From a theoretical perspective, ONNs were investigated by Winfree in mid-1960s [45], Kuramoto in mid-1970s [46] and an important mathematical analysis work was done by Crawford in early 1990s [47]. These theoretical contributions are nicely reviewed by Strogatz in

ref. [48], however the choice of MIT-based capacitors as basic blocks makes the modelling sensitive because these devices are highly non-linear and typical circuit simulators hardly handle this kind of devices. The question of the behaviour of large arrays of such non-linear devices is still open and may require new kind of simulators, able to account for chaotic behaviour of MIT-based oscillators [36, 49].

Upon this basis, the use of ONNs for information processing was more clearly described by Hoppensteadt and Izhikevich in late 1990s. The idea was to use ONNs to perform associative tasks such as pattern recognition [50]. This is done by capacitively coupling oscillators and checking their synchronisation to assess the proximity of their bias. Indeed synchronisation of oscillators is a crucial feature for the operation of ONNs. It has been widely studied because it is involved in many natural phenomena. It has been particularly suggested that synchronisation was a way for the visual cortex to distinguish an object from the background of an image [51]: the cortical neurons connected to the retinal cells receiving parts of the image that have common properties (shape, colour, movement) are synchronized. Similar operation has also been found in olfactive nervous systems of insects [52]. Mimicking such synchronization-based networks could provide very interesting applications and the most famous theoretical proposition is the associative memory network by Hoppensteadt and Izhikevich [50, 53]. The interest for this network has been renewed by studies dealing with emerging nanodevices, which are able to produce electrical oscillations, so that several attempts of practical implementations of ONNs were proposed [54]. In particular, the recent raise of studies on MIT materials triggered the publication of results on ONNs based on MIT capacitors [55-59].

At present, the exact requirements of practical circuits are being investigated. The external circuitry, which will be required as interface between oscillators and the outer world, has been proposed [60] and the parasitic impact brought about by interconnections on the characteristics of oscillators has been studied [6]. However, other questions still have to be addressed. For instance, the reliability of MIT materials after many oscillations has to be more studied because it may be an issue for applications or at least a source of device-to-device variability, as shown by early papers on this topic [44, 61]. This leads to another question of prime importance: how large can the device-to-device variability while maintaining associative properties? This variability may concern intrinsic frequency and amplitude of oscillations and RLC values of interconnects for instance. It is expected that the tolerance on variability is related to the strength of the coupling between pairs of oscillators, i.e. the value of coupling capacitances in the case of capacitive coupling. The results presented hereafter (and preliminarily reported in [59]) give an overview of the influence of coupling strength on the behaviour of pairs of oscillators.

3.2. Experimental results

VO₂ films were obtained by electron-beam evaporation from a vanadium target under oxygen atmosphere on c-cut sapphire substrate and were subsequently integrated in two-terminal planar devices fabricated as described in the work [62]. Such a device can be use either as a fast electrical switch or, within specific excitation conditions, as a relaxation oscillator [6, 63]. Typical images of the realized devices (as basic oscillator blocks) having different dimensions are presented in Fig. 7. The device images of the second row in Fig. 7 show the modification of the VO₂ material color (reflectivity) as an indication of its electrically-induced insulator-to-metal transition while applying on the planar electrodes a voltage having a value of 65 V superior to the threshold voltage initiating the MIT.

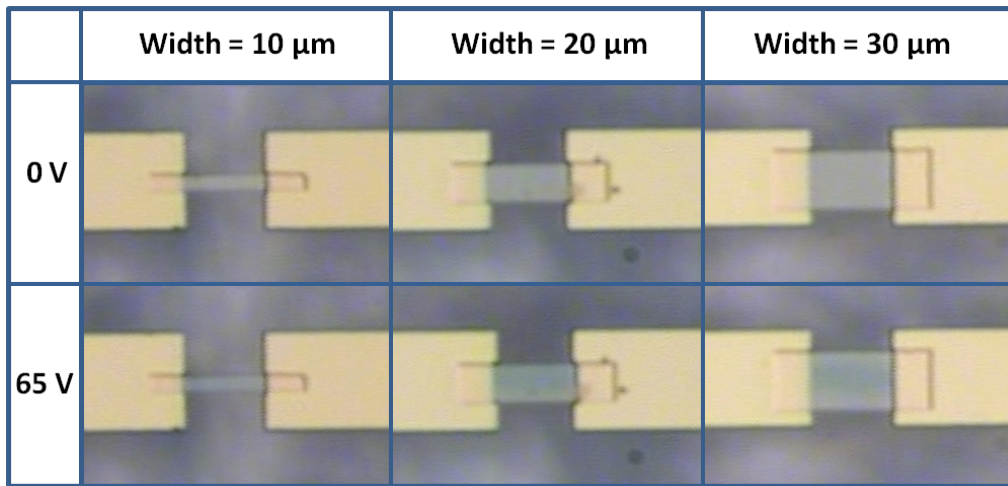


Fig. 7. Optical microscopy images of planar devices integrating VO₂ patterns with different widths (30, 20 and 10 μm) and similar length (10 μm) under two different voltages, of 0 V (material in the insulator state) and 65 V (material in the metallic state).

Depending on their geometrical parameters, on the values of the current excitation and device temperature, the frequency of these VO₂-based oscillators can be conveniently and finely adjusted within specific desired values (typically between tens of kHz up to 1 MHz [63]).

Coupling experiments may be carried out very simply by connecting a capacitor between two oscillators (noted as oscillator 1 and 2), as sketched by Fig 8(a). In the measurements presented here, an external variable capacitor (noted as C_C) was used. Each oscillator is connected to a series resistor (50 Ω) biased by a carefully chosen current (noted as I_1 and I_2 for respectively oscillator 1 and 2), in our case a Keithley 2612A current source was used. To determine the bias current, static characteristics of each oscillator is first recorded in V -mode, Fig. 8(b), and I -mode, Fig. 8(c). The NDR region is observed in I -mode characteristics between 0.25 and 2.5 mA on both devices so the current biases have to be chosen in this range to trigger oscillatory behaviors in them. Currents of respectively 1 and 1.5 mA were chosen to bias

oscillator 1 and 2, which featured very different oscillation frequencies (respectively at 3.5 and 20 kHz), as shown by Fig. 9(a). However they synchronize when a capacitor with a high enough capacitance ($C_C=100$ nF) is coupling them (Fig 9(c)). The synchrony occurs both in frequency and in phase, as shown by the phase portraits shown in Figs 9(b) and 9(d): without the capacitor, the phase portrait displays disordered points (Fig. 9(b)) whereas with the 100 nF capacitor the points gather around a right segment (Fig. 9(d)), which evidences phase-locking. Actually when

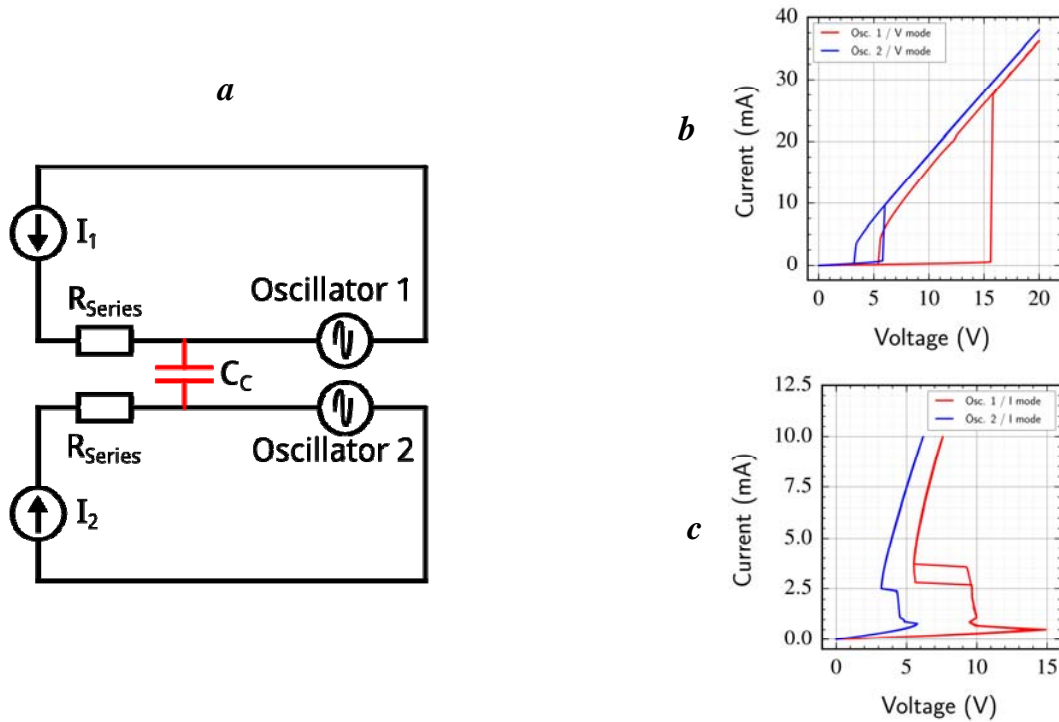


Fig. 8. Scheme (a) and I - V curves recorded in the sweep voltage (V -mode) (b) and sweep current (I -mode) (c).

the capacitance value is increased up to 100 nF, a progressive frequency locking occurs, characterized by a convergence of the oscillation frequencies of both oscillators. It is observable on oscillograms and phase portraits related to each capacitance value (see Section 5 below for supplementary data) but a convenient way to discern it is to look at the Fourier Transform of the signals as a function of the frequency (Fig. 10), which in this case shows that the final locking frequency is about 4 kHz. The coupling can be even stronger (see supplementary data for $C_C > 100$ nF in Section 5), in this case the phase portraits are more linear but then the applicative sense coupling is lost: oscillators are always synchronised whatever their bias. Neural networks instead expect weak coupling to provide useful applications such as pattern recognition [49, 50], therefore future studies should focus on values of C_C well below 100 nF.

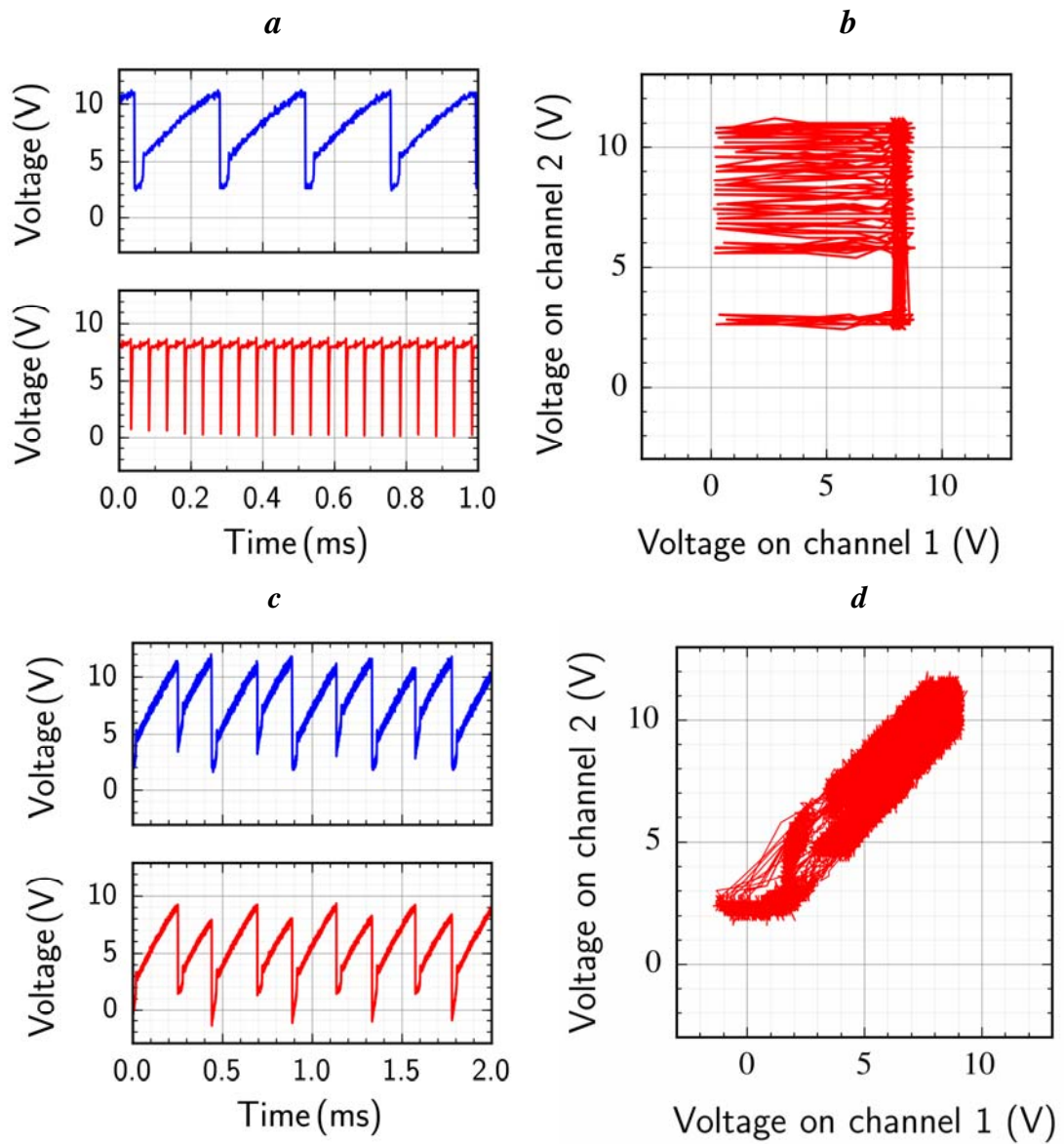


Fig. 9. Oscilloscopes (a, c) and phase portraits (b, d) of two oscillators operating in the uncoupled (a, b) and coupled (c, d) modes. Coupling capacity is $C_C = 100$ nF.

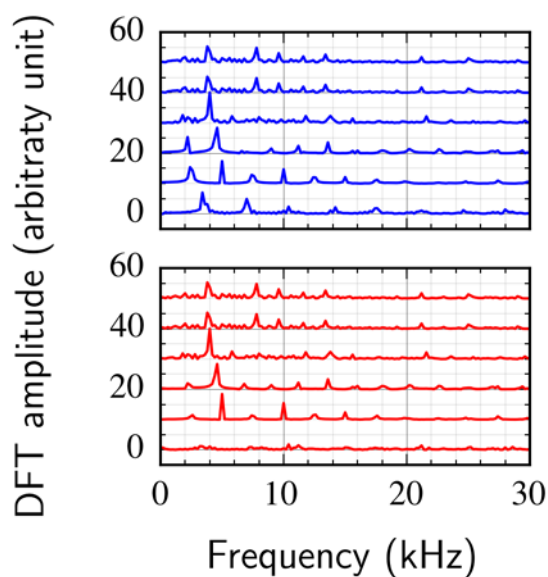


Fig. 10. Discrete Fourier Transform (DFT) of oscillations of two devices for six values of C_C (from the bottom up): 10, 50, 100, 500, 1000, and 5000 nF.

4. Conclusion and outlook

As is discussed in Section 2, vanadium dioxide undergoes the Mott MIT and the two-terminal MOM devices with VO₂ films demonstrate electronic switching associated with this transition. In electrical circuit containing such a switching device, relaxation oscillations are observed if the load line intersects the I - V curve at a unique point in the NDR region. This oscillatory behavior is prospective for designing elements of dynamical neural networks based on coupled oscillators.

We emphasize that neurocomputers offer a massively parallel computing paradigm by mimicking the human brain (see discussion in Section 3.1). Their efficient use in statistical information processing has been proposed to overcome critical bottlenecks with traditional computing schemes for applications such as image and speech processing, and associative memory [64]. In neural networks information is generally represented by phase/frequency (ONNs) or amplitude (e.g., cellular neural networks). In contrast to mature amplitude-based neural networks, nascent oscillatory neurocomputing circuits offer more efficient information processing, since they best simulate dynamical binding used in olfactory, auditory and visual systems of the brain [65].

Nonetheless, ONNs have not yet been efficiently realized on the basis of conventional CMOS devices because of large power consumption and high circuit complexity of such CMOS-based implementations which have led researchers to explore the use of emerging technologies for such circuits [64]. Although they provide intriguing properties, previously proposed ONN components based on emerging technologies have not offered a complete and practical solution to efficiently construct an entire system. For example, spin-torque oscillators (STOs) coupled with spin diffusion current [66] with electrical read-out has been proposed to construct ONNs [67]. In spite of their novelty and scalability, coupled STOs suffer from high bias currents (in the order of mA) and slower speeds that are limited by the angular spin precession velocity in nano-magnets; in addition, coupling via spin-diffusion current is low power, but localized as the spin diffusion lengths are in the order of μm at room-temperature [57]. An alternative approach is based on synchronized charge oscillations in strongly correlated electron systems [55] such as e.g. vanadium dioxide exhibiting an electronic Mott metal-insulator transition, which is currently considered as one of the most promising materials for neuromorphic oxide electronics [68]. It should be noted however that, alongside vanadium dioxide, other approaches (such as aforementioned STO or resonate body transistor oscillators (RBO) [69]) and other TMOs (for instance, Ta and Ti oxides [70]) have also being developed and considered as prospective candidate techniques for the ONN ideology implementation.

Thus, the material implementation of bio-inspired neural networks is in its infancy. The measurements presented here (Section 3.2) and a few other ones in the literature [7, 55-58] show that early demonstrations of synchronization can be performed with a few MIT materials-based oscillators. Experiments have to be done on larger arrays to assess the feasibility of basic information processing such as associative memorization or saliency recognition. Upon this basis, the impact of weak reliability and large variability should then be studied since neural networks are expected to be more able to deal with such issues than current Von-Neumann information processing architectures.

5. Supplement

In Section 3.2, the oscillograms and the phase portraits are shown for uncoupled oscillators and coupling capacitance $C_C=100$ nF. The following figures are data relative to other coupling capacitances: $C_C=10$ nF (Fig.10), 50 nF (Fig.11), 500 nF (Fig.12), 1000 nF (Fig.13) and 5000 nF (Fig.14).

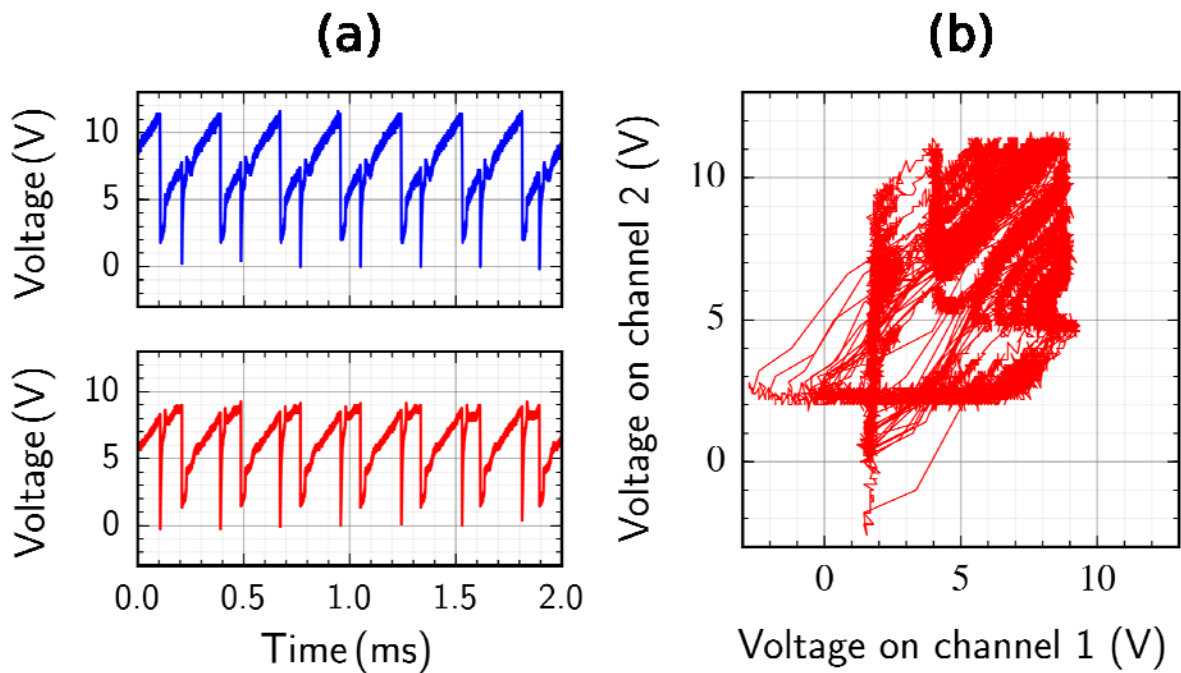


Fig. 10. (a) Oscillograms for oscillator 1 (top) and oscillator 2 (bottom) operating in the coupled mode with a coupling capacitance of $C_C = 10$ nF. (b) Phase portrait related to this coupling.

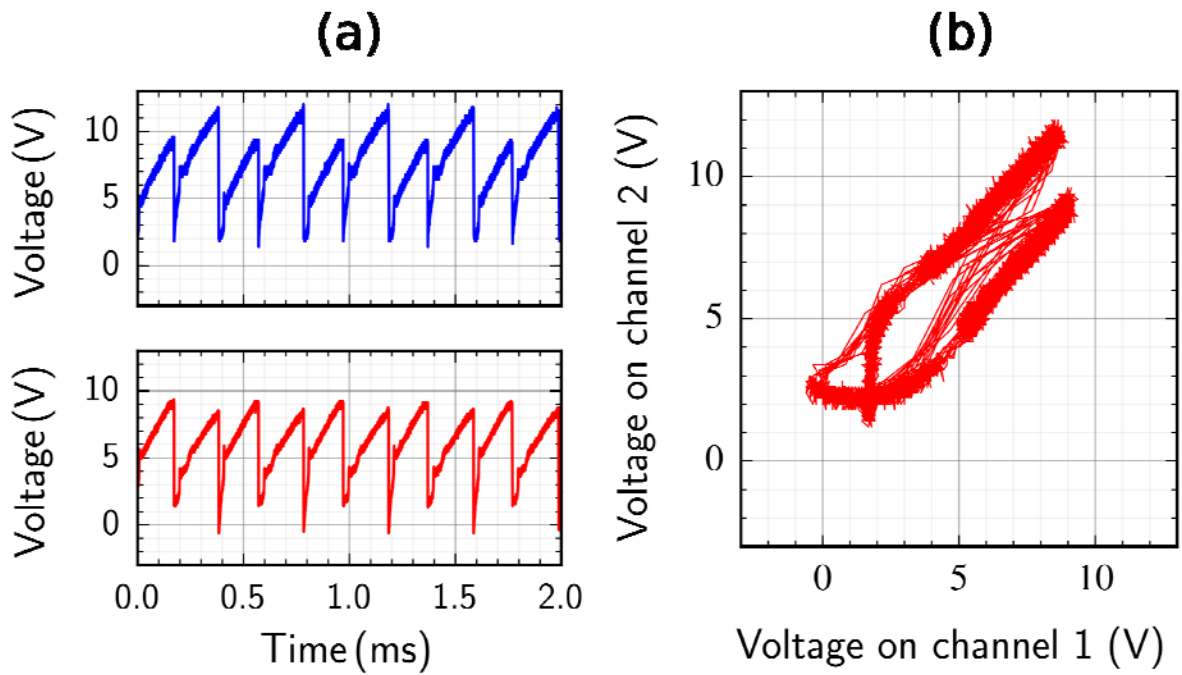


Fig. 11. (a) Oscilloscope traces for oscillator 1 (top) and oscillator 2 (bottom) operating in the coupled mode with a coupling capacitance of $C_C = 50$ nF. (b) Phase portrait related to this coupling.

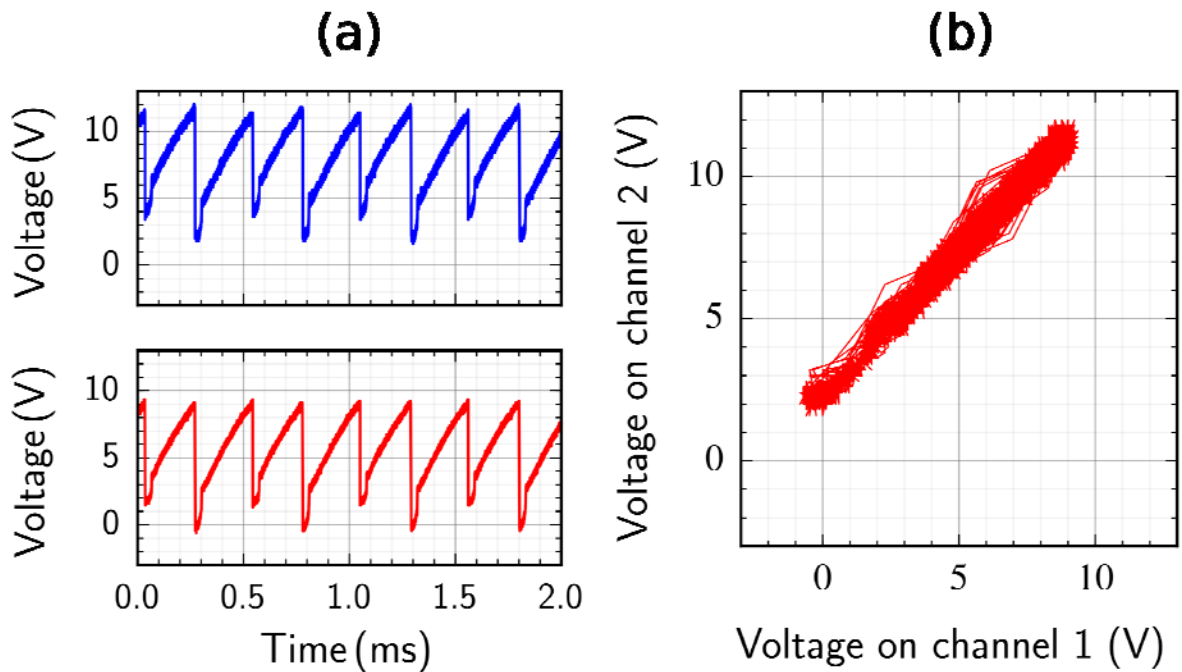


Fig. 12. (a) Oscilloscope traces for oscillator 1 (top) and oscillator 2 (bottom) operating in the coupled mode with a coupling capacitance of $C_C = 500$ nF. (b) Phase portrait related to this coupling.

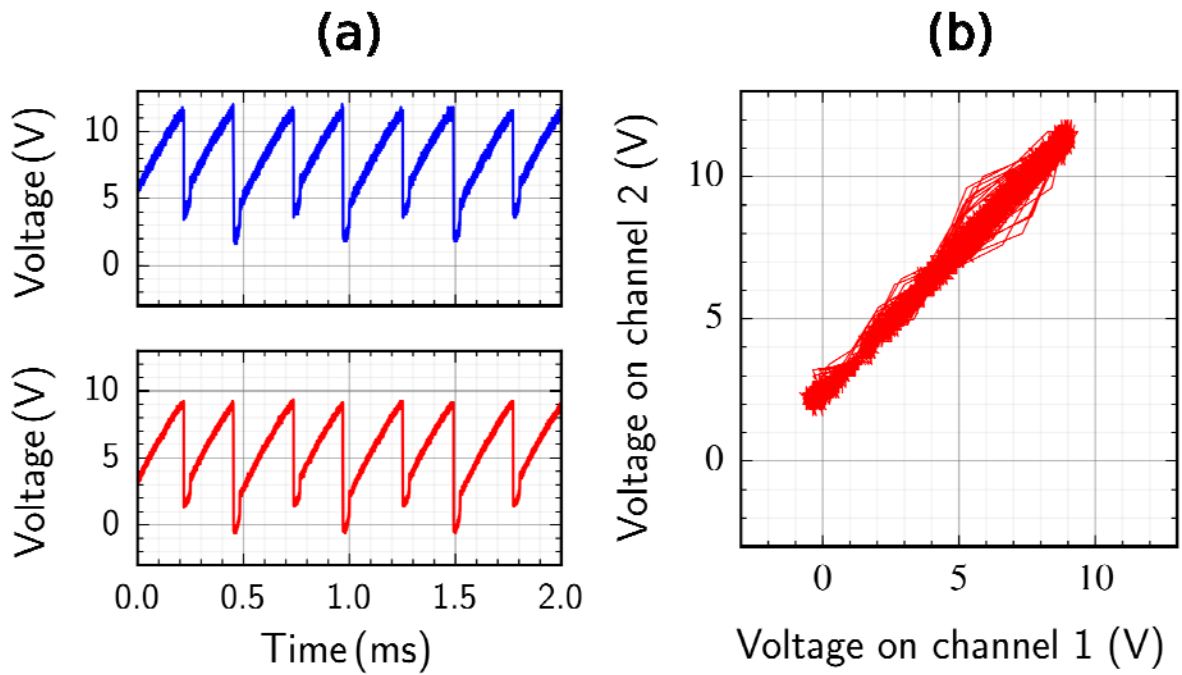


Fig. 13. (a) Oscilloscope traces for oscillator 1 (top) and oscillator 2 (bottom) operating in the coupled mode with a coupling capacitance of $C_C = 1000$ nF. (b) Phase portrait related to this coupling.

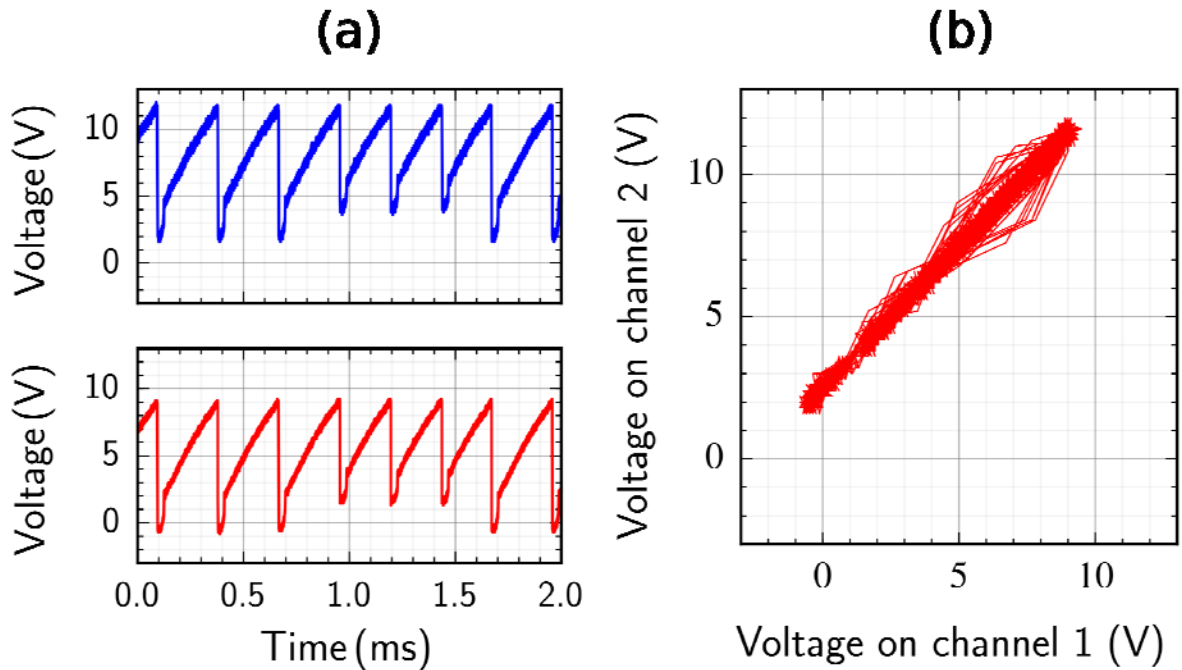


Fig. 14. (a) Oscilloscope traces for oscillator 1 (top) and oscillator 2 (bottom) operating in the coupled mode with a coupling capacitance of $C_C = 5000$ nF. (b) Phase portrait related to this coupling.

Acknowledgements

This work was partly supported by the RF Ministry of Education and Science as a base part of state Program no. 2014/154 in the scientific field, Project no. 1426, State Program no. 3.757.2014/K, and RSF grant no. 16-19-00135, (Russia). A. Pergament also acknowledges the financial support of the “Mechnikov Program” (France).

References

1. *Oxide Electronics and Functional Properties of Transition Metal Oxides* (A. Pergament, Editor), New-York: NOVA Sci. Publishers, 2014.
2. J. S. Kilby. Turning Potential into Reality: The Invention of the Integrated Circuit. Nobel Lecture, 2000. Available at http://www.nobelprize.org/nobel_prizes/physics/laureates/2000/kilby-lecture.html
3. H. Takagi and H. Y. Hwang, "An Emergent Change of Phase for Electronics," *Science* 327, 1601 (2010).
4. N. F. Mott, *Metal-Insulator Transitions*, 2nd ed. London: Taylor and Francis, 1990.
5. A. Pergament, G. Stefanovich, and A. Velichko, "Oxide Electronics and Vanadium Dioxide Perspective: A Review," *J. Sel. Top. Nano Electron. Comput.* 1, 24 (2013).
6. A. Beaumont, J. Leroy, J.-C. Orlianges, and A. Crunteanu, "Current-induced electrical self-oscillations across out-of-plane threshold switches based on VO₂ layers integrated in crossbars geometry," *J. Appl. Phys.* 115, 154502 (2014).
7. A. Parihar, N. Shukla, S. Datta, and A. Raychowdhury, "Synchronization of pairwise-coupled, identical, relaxation oscillators based on metal-insulator phase transition devices: A Model Study," *J. Appl. Phys.* 117, 054902 (2015).
8. F. J. Morin, "Oxides Which Show a Metal-to-Insulator Transition at the Neel Temperature," *Phys. Rev. Lett.* 3, 34 (1959).
9. H. J. Schlag and W. Scherber, "New sputter process for VO₂ thin films and examination with MIS-elements and C-V-measurements," *Thin Solid Films* 366, 28 (2000).
10. D. I. Khomskii, *Transition Metal Compounds*. Cambridge University Press, 2014.
11. A. Cavalleri, C. Toth, C. W. Siders, J. A. Squier, F. Raksi, P. Forget, and J. C. Kieffer, "Femtosecond structural dynamics in VO₂ during an ultrafast solid-solid phase transition," *Phys. Rev. Lett.* 87, 237401 (2001).
12. G. Stefanovich, A. Pergament, and D. Stefanovich, "Electrical switching and Mott transition in VO₂," *Journal of Physics: Condensed Matter* 12, 8837 (2000).
13. A. L. Pergament, P. P. Boriskov, A. A. Velichko, and N. A. Kuldin, "Switching effect and the metal-insulator transition in electric field," *Journal of Physics and Chemistry of Solids* 71, 874 (2010).
14. G. B. Stefanovich, A. L. Pergament, A. A. Velichko, and L. A. Stefanovich, "Anodic oxidation of vanadium and properties of vanadium oxide films," *J. Phys.: Condensed Matter* 16, 4013 (2004).
15. F. A. Chudnovskii and G. B. Stefanovich, "Metal-insulator phase transition in disordered VO₂," *J. Solid State Chem.* 98, 137 (1992).

16. R. M. Wentzcovitch, W. W. Schulz, and P. B. Allen, "VO₂: Peierls or Mott-Hubbard? A view from band theory," *Phys. Rev. Lett.* 72, 3389 (1994).
17. A. Pergament, "Metal-insulator transition: the Mott criterion and coherence length", *J. Phys.: Condensed Matter* 15, 3217 (2003).
18. B. P. Zakharchenya, V. P. Malinenko, G. B. Stefanovich, M. Yu. Terman, and F. A. Chudnovskii, "Switching in MOM structures based on vanadium dioxide," *Pisma Zh. Tekh. Fiz.* [Sov. Tech. Phys. Lett.] 11, 108 (1985).
19. F. A. Chudnovskii, "Metal-Semiconductor Phase Transition in Vanadium Oxides and Technical Applications," *Sov. Phys. Tech. Phys.* 20, 999 (1976).
20. J. Duchene, "Direct IR measurements of filament temperature during switching in vanadium oxide film devices," *J. Solid State Chem.* 12, 303 (1975).
21. A. Mansingh and R. Singh, "The mechanism of electrical threshold switching in VO₂ crystals," *J. Phys. C* 13, 5725 (1980).
22. V. N. Andreev, N. E. Timoschenko, I. M. Chernenko, and F. A. Chudnovskii, "Mechanism of formation of switching vanadate-phosphate glasses" *Zh. Tekh. Fiz.* [*J. Tech. Phys.*] 51, 1685 (1981).
23. J. K. Higgins, B. K. Temple, and J. E. Lewis, "Electrical properties of vanadate-glass threshold switches," *J. Non-Cryst. Solids* 23, 187 (1977).
24. J. G. Zhang and P. C. Eklund, "The switching mechanism in V₂O₅ gel films," *J. Appl. Phys.* 64, 729 (1988).
25. J. Bullot, O. Gallias, M. Gauthier, and J. Livage, J. "Threshold switching in V₂O₅ layers deposited from gels," *Phys. Status Solidi (a)* 71, K1 (1982).
26. Y. Taketa and R. Furugochi, "Switching and oscillation phenomena in SnO₂-VO_x-PdO ceramics," *Appl. Phys. Lett.* 31(7), 405 (1971).
27. R. L. Remke, R. M. Walser, and R. W. Bene, "The effect of interfaces on electronic switching in VO₂ thin films" *Thin Solid Films* 97, 129 (1982).
28. E. Janod, J. Tranchant, B. Corraze, M. Querré, P. Stoliar, M. Rozenberg, T. Cren, D. Roditchev, V. T. Phuoc, M.-P. Besland, and L. Cario "Resistive Switching in Mott Insulators and Correlated Systems," *Adv. Funct. Mater.* 25, 6287 (2015).
29. A. Pergament, G. Stefanovich, V. Malinenko, and A. Velichko "Electrical Switching in Thin Film Structures Based on Transition Metal Oxides," *Advances in Condensed Matter Physics* 2015, 654840 (2015).
30. A. L. Pergament, A. A. Velichko, and G. B. Stefanovich, "Addendum to "Switching effect and the metal-insulator transition in electric field" by A. L. Pergament et al. [*J. Phys.*

- Chem. Solids 71 (2010) 874],” *Journal of Physics and Chemistry of Solids* 77, 137 (2015).
31. A. Pergament, P. Boriskov, N. Kuldin, and A. Velichko, “Electrical conductivity of vanadium dioxide switching channel,” *Phys. Status Solidi B* 247, 2213 (2010).
 32. A. L. Pergament, N. A. Kuldin, G. B. Stefanovich, and A. A. Velichko, “Dielectric properties of vanadium dioxide and perspectives of applications of the sandwich structures on the basis of VO₂ in sensor material,” *Modern problems of science and education*. № 5, 2014. <http://www.science-education.ru/en/119-r14950> .
 33. L. A. L. de Almeida, G. S. Deep, A. M. N. Lima, and H. Neff, “Thermal dynamics of VO₂ films within the metal–insulator transition,” *Appl. Phys. Lett.* 77, 4365 (2000).
 34. Z. Topalian, S.-Y. Li, G. A. Niklasson, C. G. Granqvist, and L. B. Kish, “Resistance noise at the metal–insulator transition in thermochromic VO₂ films,” *J. Appl. Phys.* 117, 025303 (2015).
 35. V. Y. Zerov, Yu. V. Kulukov, V. N. Leonov, V. G. Malyarov, I. A. Khrebtov, and I. I. Shaganov, “Features of operation of the bolometer on the basis of vanadium dioxide film in temperature range including phase transition,” *J. Opt. Technol.* 66, 387 (1999).
 36. A. A. Velichko, A. L. Pergament, G. B. Stefanovitch, and P. P. Boriskov, “Nonlinear Phenomena and Deterministic Chaos in Systems with Vanadium Dioxide,” *J. Sel. Top. Nano Electron. Comput.* 2, 20 (2014).
 37. The International Technology Roadmap for Semiconductors - 2011 Edition, Process Integration, Devices & Structures, Available at <http://www.itrs.net/Links/2011ITRS/2011Chapters/2011PIDS.pdf>
 38. The International Technology Roadmap for Semiconductors - 2011 Edition, Emerging Research Materials, Available at <http://www.itrs.net/Links/2011ITRS/2011Chapters/2011ERM.pdf>
 39. The International Technology Roadmap for Semiconductors - 2011 Edition, Emerging Research Devices, Available at <http://www.itrs.net/Links/2011ITRS/2011Chapters/2011ERD.pdf>
 40. S. Levitan, Y. Fang, D. Dash, T. Shibata, D. Nikonov, and G. Bourianoff, “Non-Boolean associative architectures based on nano-oscillators,” *Proceedings of the 13th International Workshop on Cellular Nanoscale Networks and Their Applications (CNNA)*, pp. 1–6 (2012)
 41. D. Kuzum, S. Yu, and H. S. P. Wong, “Synaptic electronics: materials, devices and applications,” *Nanotechnology* 24(38), 382001 (2013).

42. Y. W. Lee, B. J. Kim, J. W. Lim, S. J. Yun, S. Choi, B. G. Chae, G. Kim, and H. T. Kim, "Metal-insulator transition-induced electrical oscillation in vanadium dioxide thin film," *Appl. Phys. Lett.* 92(16), 162903 (2008).
43. J. Sakai, "High-efficiency voltage oscillation in VO₂ planer-type junctions with infinite negative differential resistance," *J. Appl. Phys.* 103(10), 103708 (2008).
44. A. Crunteanu, J. Givernaud, J. Leroy, D. Mardivirin, C. Champeaux, J. C. Orlianges, A. Catherinot, and P. Blondy, "Voltage- and current-activated metal-insulator transition in VO₂ -based electrical switches: a lifetime operation analysis" *Sci. Technol. Adv. Mater.* 11(6), 065002 (2010).
45. A. T. Winfree, "Biological rhythms and the behavior of populations of coupled oscillators," *Journal of Theoretical Biology* 16(1), 15 (1967).
46. Y. Kuramoto, "Self-entrainment of a population of coupled non-linear oscillators". In: H. Araki (editor) *International Symposium on Mathematical Problems in Theoretical Physics*, volume 39 of Lecture Notes in Physics, pp. 420–422. Berlin: Springer, 1975.
47. J. Crawford, "Amplitude expansions for instabilities in populations of globally-coupled oscillators," *Journal of Statistical Physics* 74(5-6), 1047 (1994).
48. S. H. Strogatz, "From Kuramoto to Crawford: exploring the onset of synchronization in populations of coupled oscillators," *Physica D: Nonlinear Phenomena* 143, 1 (2000).
49. F. Corinto, M. Bonnin, and M. Gilli, "Weakly Connected Oscillatory Network Models For Associative And Dynamic Memories," *International Journal of Bifurcation and Chaos* 17(12), 4365 (2007).
50. F. C. Hoppensteadt and E. M. Izhikevich, "Oscillatory Neurocomputers with Dynamic Connectivity," *Phys. Rev. Lett.* 82, 2983 (1999).
51. C. M. Gray, P. Konig, A. K. Engel, and W. Singer, "Oscillatory responses in cat visual cortex exhibit inter-columnar synchronization which reflects global stimulus properties," *Nature* 338(6213), 334 (1989).
52. G. Laurent and H. Davidowitz, "Encoding of Olfactory Information with Oscillating Neural Assemblies," *Science* 265(5180), 1872 (1994).
53. E. M. Izhikevich, "Computing with Oscillators," Unpublished (2000). Available at <http://citeseerx.ist.psu.edu/viewdoc/summary?doi=10.1.1.33.1937>
54. M. Cotter, Y. Fang, S. Levitan, D. Chiarulli, and V. Narayanan, "Computational Architectures Based on Coupled Oscillators," In *Proceedings of the IEEE Computer Society Annual Symposium on VLSI (ISVLSI)*, pp. 130–135 (2014).
55. N. Shukla, A. Parihar, E. Freeman, H. Paik, G. Stone, V. Narayanan, H. Wen, Z. Cai, V. Gopalan, R. Engel-Herbert, D. G. Schlom, A. Raychowdhury, and S. Datta,

- “Synchronized charge oscillations in correlated electron systems,” *Sci. Rep.* 4, 4964, (2014).
56. N. Shukla, A. Parihar, M. Cotter, M. Barth, X. Li, N. Chandramoorthy, H. Paik, D. Schlom, V. Narayanan, A. Raychowdhury, and S. Datta, “Pairwise coupled hybrid vanadium dioxide-MOSFET (HVFET) oscillators for non-boolean associative computing,” In *Proceedings of the IEEE International Electron Devices Meeting (IEDM)*, pp. 28.7.1–28.7.4 (2014).
57. S. Datta, N. Shukla, M. Cotter, A. Parihar, and A. Raychowdhury, “Neuro Inspired Computing with Coupled Relaxation Oscillators,” In *Proceedings of the The 51st Annual Design Automation Conference on Design Automation Conference, DAC '14*, pp. 74:1–74:6 (2014).
58. P. Maffezzoni, L. Daniel, N. Shukla, S. Datta, and A. Raychowdhury, “Modeling and Simulation of Vanadium Dioxide Relaxation Oscillators,” *IEEE Transactions on Circuits and Systems* 62, 2207 (2015).
59. A. Beaumont, J.-C. Orlianges, A. Boulle, A. Pergament, and A. Crunteanu, “Switching and oscillations in vanadium dioxide based devices for neuromorphic function implementation,” In *Workshop on Oxide Electronics 22, Paris - October 7-9, 2015, Book of Abstracts*, p. 179, (2015).
60. T. Shibata, R. Zhang, S. Levitan, D. Nikonov, and G. Bourianoff, “CMOS supporting circuitries for nano-oscillator-based associative memories,” In *Proceedings of the Cellular 13th International Workshop on Nanoscale Networks and Their Applications (CNNA)*, pp. 1–5 (2012).
61. C. Ko and S. Ramanathan, “Stability of electrical switching properties in vanadium dioxide thin films under multiple thermal cycles across the phase transition boundary,” *J. Appl. Phys.* 104(8) 086105 (2008).
62. J. Leroy, A. Bessaudou, F. Cosset, and A. Crunteanu, “Structural, electrical and optical properties of thermochromic VO₂ thin films obtained by reactive electron beam evaporation,” *Thin Solid Films* 520, 4823 (2012).
63. J. Leroy, A. Crunteanu, J. Givernaud, J.-C. Orlianges, C. Champeaux, and P. Blondy, “Generation of electrical self-oscillations in two-terminal switching devices based on the insulator-to-metal phase transition of VO₂ thin films,” *International Journal of Microwave and Wireless Technologies* 4(01), 101 (2012).
64. V. Calayir, *Neurocomputing and Associative Memories Based on Emerging Technologies: Co-optimization of Technology and Architecture* (Ph. D. Thesis) Carnegie

- Mellon University (2014). Available at:
<http://repository.cmu.edu/cgi/viewcontent.cgi?article=1422&context=dissertations>
65. M. G. Kuzmina, E. A. Manykin, E. S. Grichuk, *Oscillatory Neural Networks: In Problems of Parallel Information Processing*. Berlin-Boston: Walter de Gruyter GmbH (2014).
 66. T. Taniguchi, T. Ito, Y. Utsumi, S. Tsunegi, and H. Kubota “Stable oscillation in spin torque oscillator excited by a small in-plane magnetic field,” *J. Appl. Phys.* 118, 053903 (2015).
 67. S. Kaka, M. R. Pufall, W. H. Rippard, T. J. Silva, S. E. Russek, and J. Katine, “Mutual phase-locking of microwave spin torque nano-oscillators,” *Nature* 437 (7057), 389 (2005).
 68. Y. Zhou and S. Ramanathan” Mott Memory and Neuromorphic Devices,” *Proceedings of the IEEE* 103 (8), 1289 (2015).
 69. Y. Fang, V. V. Yashin, D. M. Chiarulli, and S. P. Levitan, “A Simplified Phase Model for Oscillator Based Computing,” In: *ISVLSI : IEEE Computer Society*, pp. 231-236 (2015).
 70. A. A. Sharma, J. A. Bain, and J. A. Weldon, “Phase Coupling and Control of Oxide-Based Oscillators for Neuromorphic Computing,” *IEEE Journal on Exploratory Solid-State Computational Devices and Circuits* 1, 58 (2015).